33RD INTERNATIONAL COSMIC RAY CONFERENCE, RIO DE JANEIRO 2013
THE ASTROPARTICLE PHYSICS CONFERENCE

ICRC 2013

High precision measurement of the AMS-RICH aerogel refractive index with cosmic ray

W. GILLARD[1] FOR THE AMS02-RICH COLLABORATION.

[1] *Laboratoire de Physique Subatomique et de Cosmologie (LPSC), Université Joseph Fourier Grenoble 1, CNRS/IN2P3, Institut Polytechnique de Grenoble, France*

gillard@lpsc.in2p3.fr

Abstract: AMS-02 was successfully installed on the international space station (ISS) during May 2011 and it has been taking data since. AMS-02 is devoted to precise measurements of Galactic cosmic rays of energy ranging from 100 MV to a few TV of magnetic rigidity. To identify and measure the particle properties, AMS-02 is composed of various sub-detectors. Among them, the Ring Imager Čerenkov (RICH) counter, composed of aerogel/NaF radiator planes and a detection plane, measures the velocity and absolute charge of incoming cosmic rays. Precise measurements of the particle velocity require the aerogel refractive index to be known with a precision of the order of $\Delta n/n \leq 1.5 \times 10^{-4}$. We present a method to perform in-flight measurement of the refractive index, and the mapping of the aerogel radiator plan of the AMS-RICH, directly from cosmic rays. We also discuss the time stability of the aerogel refractive index and the subsequent velocity measurements.

Keywords: Cosmic Rays, Measurement, Methods, Detectors, Čerenkov radiation, RICH, AMS

1 Description of the AMS-RICH detector

The RICH (Ring Imaging Čerenkov) is one of the AMS-02 sub-detectors, and it is devoted to precise measurements of the velocity and absolute charge of the incoming cosmic rays. As seen on the schematic view of the RICH in Fig. 1, the RICH is composed of a radiator plane inducing Čerenkov radiation, and a detection plane located 469 mm below collecting the Čerenkov light. The volume between the radiator and the detection plane is surrounded by a conical mirror to prevent Čerenkov light losses [4, 7, 10, 11].

The central part of the radiator plane is composed of 16 squared tiles (8.6×8.6 cm^2) of Sodium Fluoride (NaF) with thickness of 0.5 cm. This central part represents 10% of the radiator acceptance. The refractive index of $\simeq 1.334$ permits the detection of particles with velocity $\beta \gtrsim 0.75$. The outer part of the radiator plane represents 90% of the radiator acceptance. It is built up of 92 silica (SiO_2) aerogel tiles (thereafter AGL) which were manufactured by the Budker Institute of Novosobirsk [12, 13]. Among them, 60 have squared shape of 11.4×11.4 cm^2 while the remaining 32 tiles (located at the edge of the radiator plane) are truncated squares. Ground measurements of the AGL refractive index [4, 14] gave an average value of $\simeq 1.05$, permitting the detection of particles with velocity $\beta \gtrsim 0.95$.

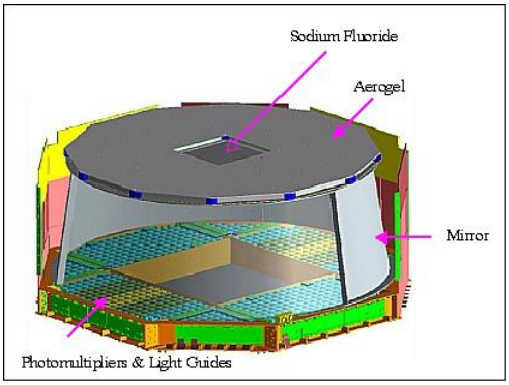

Fig. 1: Schematic view of the AMS-02 RICH.

The RICH was designed to achieve a velocity resolution $\Delta\beta/\beta \simeq 1.5 \times 10^{-4}$ for $Z > 2$ particle [6], which then required to know the refractive index of the AGL tiles with a precision better than $\Delta n/n \simeq 1.5 \times 10^{-4}$.

AGL tiles are hydrophilic and their physical properties vary with variation of the atmospheric humidity and pressure. Therefore, ground measurements were performed under controlled dry nitrogen atmosphere [4, 14]. Once AMS-02 was installed onto the ISS, the nitrogen gas filling up the AGL container naturally evaporated in outer space, resulting in variations of tile's refractive index. To account for this variation, in-flight calibration of the AGL refractive index was necessary. Below, we present an in-flight method used to map and calibrate the refractive index of the AGL tiles of the AMS-RICH sub-detector, using cosmic rays themselves. We also discuss the stability of the velocity measurements provided by the AMS-RICH sub-detector.

2 Mapping the AGL refractive index

2.1 Method

Cosmic-ray protons of magnetic rigidity $R > 10$ GV are pre-selected by requiring that the deposited energies from ionisation/excitation (measured in both the AMS-02 tracker and the Time of Flight sub-detectors [2, 1, 5, 3]) are compatible with charge $Z = 1$ particles. Assuming that the incoming cosmic ray is a proton, we calculate its expected velocity (β_0), based on the magnetic rigidity (R) deduced from the particle curvature measured within the AMS-tracker [8]:

$$\beta_0 = \frac{R}{m_p} \times \left(\frac{R^2}{m_p^2} - 1 \right)^{-1/2} , \qquad (1)$$

m_p being the proton mass in GeV.

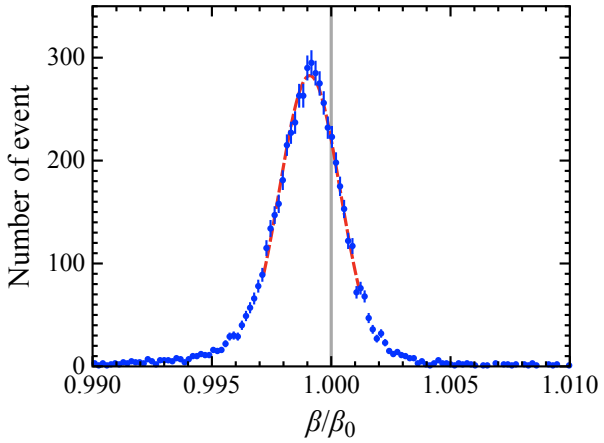

Fig. 2: Measured-to-Expected velocity ratio distribution obtained from $R > 10$ GV protons passing through a 0.5×0.5 cm^2 section of the whole RICH surfaces (*blue symbols*). The gaussian fit of the distribution (*red dashed line*) and the reference value $\beta/\beta_0 = 1$ (*gray line*) are also shown.

Meanwhile, protons crossing the AGL radiator plan produce Čerenkov cones that are projected on the RICH detection plane. Using the AMS-tracker measurements, the spatial distribution of the detected Čerenkov photons and the particle incident angle and position (of its impact points onto the radiator plane) are combined to infer the Čerenkov angle (θ_c) and, subsequently, to estimate the incoming-particle velocity:

$$\beta = \frac{1}{n_0(x,y) \times \cos\theta_c} \qquad (2)$$

with $n_0(x,y)$ the on-ground measured AGL refractive index [4, 14] at the particle impact point coordinates (x,y).

Considering a large protons sample of rigidity $R >$ 10 GV, we studied the measured-to-expected velocity ratio distribution. An example is shown in Fig. 2 for a small portion of the whole AGL surface. This distribution has a gaussian shape with a width determined by the uncertainties on the RICH velocity and Tracker rigidity measurements.

Assuming that the refractive index of each AGL tile does not varies with time, one would expect that the measured-to-expected velocity ratio distribution picks at a value $\beta/\beta_0 =$ 1. Any displacement of the distribution's center with respect to the expected value means that a new calibration is required. The calibrated value for the refractive index is obtained from

$$n(x,y) = n_0(x,y) \times \langle \frac{\beta}{\beta_0} \rangle \qquad (3)$$

with $\langle \beta/\beta_0 \rangle$ the mean position of the measured-to-expected velocity ratio derived from a gaussian fit of the distribution (see Fig. 2).

2.2 Calibration and precision

AGL tiles have an average thickness of $\simeq 2.5$ cm, with a thickness 0.3 to 0.5 mm larger near the border than at its center. As we are not able measure the depth at which the Čerenkov radiation is emitted, the thickness of the AGL tile are source of uncertainties in the measurement

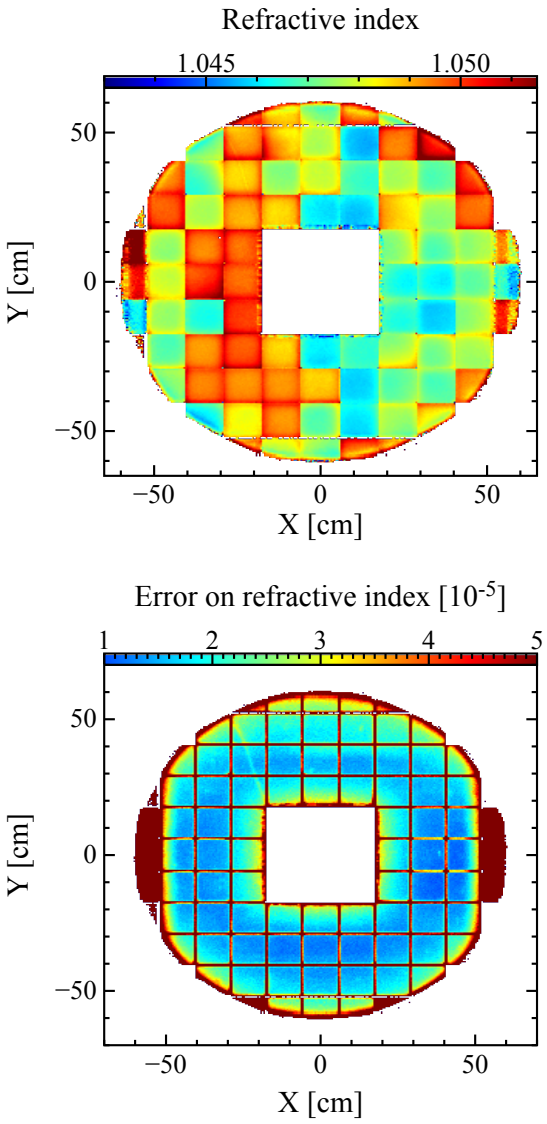

Fig. 3: Color-coded maps of the RICH-AGL refractive index (top) and its uncertainties (bottom). The points in the maps are calculated on a spacial grid of 0.5×0.5 cm^2

of the refractive index. Thus, we present measurement of the refractive index averaged over the particle path length through the AGL tile.

The top panel in Fig. 3 show the map of the AGL refractive index, derived from AMS-02 in-flight data recorded between July 2011 and July 2012. Thanks to the high statistics of AMS-02 events, the spatial resolution is much better than the tile size: we subdivided each of the 92 AGL tiles into a spacial grid of 0.5×0.5 cm^2. Different AGL tiles have a different density, and therefore a different refractive index. Also, within a single tile, we can clearly distinguish the index gradient which is due to a non-homogeneous density. The bottom panel in Fig. 3 shows the map of the AGL refractive index uncertainty: the precision reached is a few 10^{-5}. When a particle passes near the edge of a tiles, a fraction of the emitted Čerenkov photon is absorbed by the wall (which isolates the tiles from one another). This reduces the accuracy of the particle velocity reconstruction, therefore the precision on the AGL refractive index on the edge of the

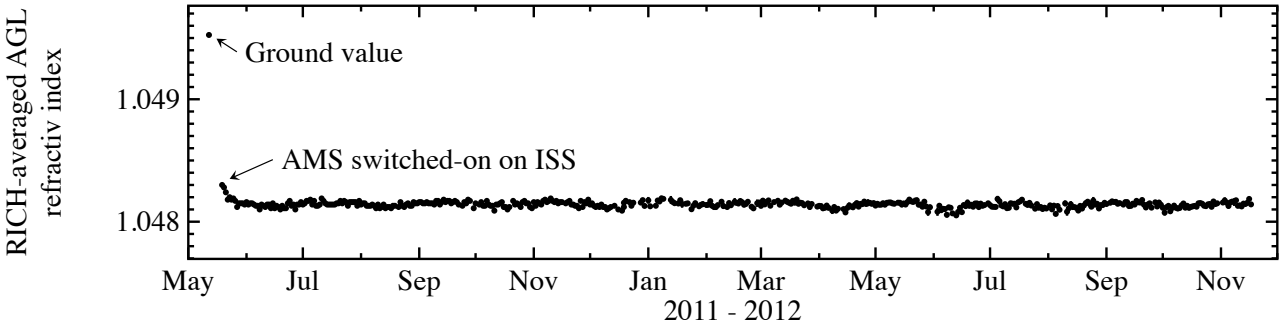

Fig. 4: Evolution of the AMS refractive index over time

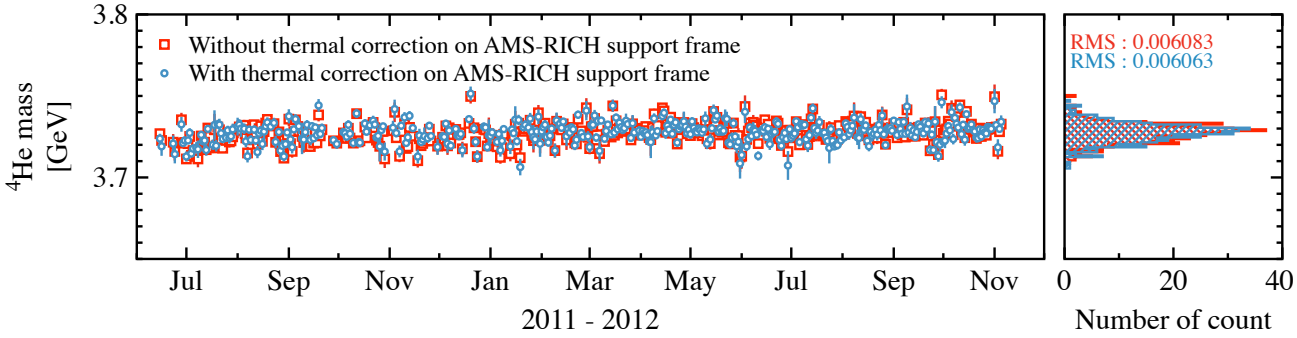

Fig. 5: Left panel: evolution of the ^{4}He-mass measurement over time before (*red open squares*) and after (*blue open circles*) applying the correction on the distance between the radiator and the detection plane of the RICH. Right panel: overall distribution of the ^{4}He-mass pic measured before (*red*) and after (*blue*) applying the correction.

radiation plane as well as at the border of each tile worsen.

2.3 Checks

A possible bias could come from miss-reconstructed rigidities. Indeed, a wrong measurement of the particle rigidity would bias our estimation of the expected velocity deduced from Eq. (1): it would introduce an artificial shift in the measured-to-expected velocity ratio. To control our systematics on the refractive index calibration, we repeated the procedure for protons of rigidity $R > 100$ GV for which the expected velocity is 0.99996. Given the RICH velocity resolution $\Delta\beta/\beta \simeq 1.2 \times 10^{-3}$ for $Z = 1$ particle, it is safe to assume $R > 100$ GV protons have a velocity $\beta \simeq 1$ [Eq. (1) is then not used]. The refractive index, averaged over all RICH tiles, is found to be $1.048149 \pm (6 \times 10^{-6})$ for $R > 100$ GV. This is compatible with the averaged refractive index of $1.048144 \pm (2 \times 10^{-6})$ obtained for $R > 10$ GV protons.

3 Time stability of the AGL refractive index

In addition to the mapping of the AGL refractive index, we also monitored the time variation of the refractive index, relying on the method described in Section 2. To accumulate enough statistic, we consider the whole radiator plane on a daily basis.

3.1 Time evolution

Figure 4 shows the evolution of the refracting index with time. First, it is important to highlight the difference (about 1.5×10^{-3}) observed between ground and in-flight measurements. It is due to the evaporation of the nitrogen gas which filled up the AGL tiles container to keep them in dry hydrogen and stable conditions while it was on the ground. It took approximately one week before all the nitrogen leaked out in space. Afterward, the AGL refractive index stabilised around a mean value (over all tiles) of 1.04814.

3.2 Impact of thermal effects on the determination of AGL refractive index

In Fig. 4, we still observe fluctuation at the level of $\Delta n \simeq 10^{-5}$ after June 2011 caused by thermal effects. Indeed, in space, AMS-02 suffers severe temperature changes which deform the AMS-02 structure. In the case of the RICH sub-detector, these thermal variations slightly modify the distances between the radiator and the detection planes. If not corrected, this biases the RICH velocity measurement and subsequently our estimation of the refractive index. Thermal effects on the AMS-RICH support frame can be monitored and corrected from the alignment of the layer 9 of the silicon tracker which is fixed on the same support as the RICH detection plane [9]. We then reconstructed the helium mass (which is a proxy for the AGL refractive index) with and without this correction (red squares and blue circles in the left panel of Fig. 5). Comparing the ^{4}He mass we measure (see right panel on Fig. 5), we see the temperature fluctuations does not significantly affect the resolution of the helium mass, therefore, the physics inferred from the RICH measurements.

4 Conclusion

A precise knowledge of the AGL refractive index is necessary to precisely infer the velocity (as well as the absolute charge) of incoming charged particles emitting Čerenkov radiation while crossing the RICH's AGL radiator plane. We have presented a method allowing to measure and monitor in space the RICH AGL refractive index from the velocity measurement of the cosmic rays themselves.

It is important to highlight that the refractive index we measured in space is 1.5×10^{-3} smaller than that measured on ground. This variation is larger than the scientific requirement $\Delta n/n \lesssim 1.5 \times 10^{-4}$ to precisely measure the particle velocity and charge with the RICH. Therefore, it was mandatory to have in-flight calibration. Thanks to the statistic accumulated so far by the AMS-02 experiment, we are able to produce high precision maps of the AGL tiles with a precision of $\Delta n/n \simeq 2 \times 10^{-5}$ on average.

Acknowledgment: We acknowledge the continuous support from CNRS, IN2P3, CNES, Enigmass, the ANR, France; Foundation for Science and Technology, Portugal; CIEMAT, CDTI, SEIDI-MINECO, and CPAN, Spain.

References

[1] A. Basili *et al.*, Nuclear Instruments and Methods in Physics Research Section A: Accelerators, Spectrometers, Detectors and Associated Equipment, 2013, **707**:99 – 113.
[2] B. Alpat *et al.*, Nuclear Instruments and Methods in Physics Research Section A: Accelerators, Spectrometers, Detectors and Associated Equipment, 2010, **613**:207 – 217.
[3] K. Lübelsmeyer *et al.*, Nuclear Instruments and Methods in Physics Research Section A: Accelerators, Spectrometers, Detectors and Associated Equipment, 2011, **654**:639 – 648.
[4] M. Aguilar-Benitez *et al.*, Nuclear Instruments and Methods in Physics Research Section A: Accelerators, Spectrometers, Detectors and Associated Equipment, 2010, **614**:237 – 249.
[5] V. Bindi *et al.*, Nuclear Instruments and Methods in Physics Research Section A: Accelerators, Spectrometers, Detectors and Associated Equipment, 2010, **623**:968 – 981.
[6] P. Aguayo *et al.*, Nuclear Instruments and Methods in Physics Research A, 2006, **560**:291–302.
[7] M. Aguilar-Benitez, L. Arruda, F. Barao, and et al.: 2008, in *International Cosmic Ray Conference* Vol. 2 of *International Cosmic Ray Conference* 461–464.
[8] G. Ambrosi *et al.*, in 33^{rd} International Cosmic Ray Conferences, 2013, **Abstract ID**:1064.
[9] G. Ambrosi *et al.*, in 33^{rd} International Cosmic Ray Conferences, 2013, **Abstract ID**:1260.
[10] L. Arruda, F. Barão, P. Gonçalves, and R. Pereira, Nuclear Physics B Proceedings Supplements, 2007, **172**:32–35.
[11] D. Casadei, Nuclear Physics B Proceedings Supplements, 2003, **125**:303–307.
[12] A. Danyliuk *Budker Institute of Novosobirsk* private communication.
[13] E. Kravtechenko and A. Onuchin *Budker Institute of Novosobirsk* private communication.
[14] Y. Sallaz-Damaz *et al.*, Nuclear Instruments and Methods in Physics Research A, 2010, **614**:184–195.